Korean J Hepatobiliary Pancreat Surg 2015;19:47-58
http://dx.doi.org/10.14701/kjhbps.2015.19.2.47

Original Article

Toward angiogenesis of implanted bio-artificial liver using scaffolds with type I collagen and adipose tissue-derived stem cells

Jae Geun Lee[1], Seon Young Bak[2], Ji Hae Nahm[3], Sang Woo Lee[1,2], Seon Ok Min[1,2], and Kyung Sik Kim[1,2,4]

[1]Department of Surgery, Yonsei University College of Medicine, [2]Graduate Program of Nano Science and Technology, Graduate School of Yonsei University, [3]Department of Pathology, Yonsei University College of Medicine, [4]Cell Therapy Center, Severance Hospital, Seoul, Korea

Backgrounds/Aims: Stem cell therapies for liver disease are being studied by many researchers worldwide, but scientific evidence to demonstrate the endocrinologic effects of implanted cells is insufficient, and it is unknown whether implanted cells can function as liver cells. Achieving angiogenesis, arguably the most important characteristic of the liver, is known to be quite difficult, and no practical attempts have been made to achieve this outcome. We carried out this study to observe the possibility of angiogenesis of implanted bio-artificial liver using scaffolds. **Methods:** This study used adipose tissue-derived stem cells that were collected from adult patients with liver diseases with conditions similar to the liver parenchyma. Specifically, microfilaments were used to create an artificial membrane and maintain the structure of an artificial organ. After scratching the stomach surface of severe combined immunocompromised (SCID) mice (n=4), artificial scaffolds with adipose tissue-derived stem cells and type I collagen were implanted. Expression levels of angiogenesis markers including vascular endothelial growth factor (VEGF), CD34, and CD105 were immunohistochemically assessed after 30 days. **Results:** Grossly, the artificial scaffolds showed adhesion to the stomach and surrounding organs; however, there was no evidence of angiogenesis within the scaffolds; and VEGF, CD34, and CD105 expressions were not detected after 30 days. **Conclusions:** Although implantation of cells into artificial scaffolds did not facilitate angiogenesis, the artificial scaffolds made with type I collagen helped maintain implanted cells, and surrounding tissue reactions were rare. Our findings indicate that type I collagen artificial scaffolds can be considered as a possible implantable biomaterial. **(Korean J Hepatobiliary Pancreat Surg 2015;19:47-58)**

Key Words: Tissue scaffolds; Liver; Artificial; Neovascularization; Physiologic; Biocompatible materials

INTRODUCTION

There is an extreme worldwide lack of transplantable organs, and many patients are on waiting lists. According to 2013 data from the Korean Network for Organ Sharing (KONOS), there were 13,689 and 4,263 patients waiting for kidney and liver transplantations, respectively.[1] These numbers are increasing by approximately 20% annually, but the numbers of donors remain flat. In 2013, just 1,351 of the 4,263 patients received liver transplantation, but less than one-third were deceased donor transplants.[1]

This demand and supply mismatch of organs is a persistent worldwide problem,[2-4] and although many studies have been carried out to identify viable alternatives to deceased donor organs, these projects remain in the early stages.[5] Part of this effort is a liver support system that is largely categorized into two systems. The first is an artificial liver support system that mainly focuses on detoxification also known as the Molecular Absorbent Recirculating System (MARS^{TM}), and the second is a bio-artificial liver support system that detoxifies and has synthetic and regulatory functions. Unfortunately, these systems are extremely expensive, and problems with the membrane and biocompatibility make it unlikely that these solutions will be clinically viable.[6-8]

Hepatocyte transplantation is another alternative. The donor's hepatocytes are integrated into the recipient's liver following their insertion into the portovenous system and

Received: May 2, 2015; **Revised:** May 25, 2015; **Accepted:** May 28, 2015
Corresponding author: Kyung Sik Kim
Department of Surgery, Yonsei University College of Medicine, 134 Shinchon-dong, Seodaemun-gu, Seoul 120-752, Korea
Tel: +82-2-2228-2125, 2100, Fax: +82-2-313-8289, E-mail: kskim88@yuhs.ac

subsequent translocation to the hepatic sinusoids.[9-11] This approach has been reported to be clinically effective in congenital metabolic diseases. For example, serum bilirubin levels are reportedly decreased by 25-50% after hepatocyte transplantation in patients with Crigler-Najjar syndrome.[12-16] However, the effect decreased with time, and patients eventually required whole liver transplantation due to hepatocyte graft failure after 4-48 months.

Regarding functional cell differentiation, there have been reports of endothelial cells producing dopamine,[17] pancreatic cells secreting insulin,[18] and cells functioning as hepatocytes.[19] In addition, cells differentiated from autologous cells that function as hepatocytes have been transplanted into human recipients,[20] but the lack of angiogenesis associated with these functional differentiated cells remains problematic.

Vasculogenesis and angiogenesis are unique processes. The former is the formation of primary capillary blood vessels from mesodermal cells that first differentiate into angioblasts and then endothelial cells.[21] Angiogenesis involves the sprouting of new vessels from existing vessels.[21] This is a complex process that involves basement membrane degradation and proliferation, migration, and endothelial cell tube formation. Angiogenesis is critical for the development and wound healing of normal tissue, as well as ensuring adequate oxygen and nutrient supplies to transplanted tissues.[22]

Angiogenesis is stimulated by hypoxia-inducible factors (HIFs) and the expression of many other signals including vascular endothelial growth factor (VEGF), platelet-derived growth factor (PDGF), and angiopoietin2 (Ang2).[23] VEGF is a signaling peptide that facilitates angiogenesis,[24] and immunohistochemical labeling of this protein has been used as a histological assessment tool.[25-27] It increases the permeability of endothelial cells and facilitates the creation of new vessels.[28] When overexpressed, it can facilitate the development of cancer, atherosclerosis, rheumatic arthritis, diabetic retinopathy, and so on.[29,30]

Other proteins such as CD31, CD34, CD105, and von Willebrand factor (vWF) also play important roles in angiogenesis. CD34 is a 110-kDa transmembrane glycoprotein expressed in white blood cells, endothelial cells, and stem cells. It can also be found around the splenic marginal zone and in dendritic cells in vessels, nerves, sweat glands, and hair pouches.[31,32] The function of CD34 is not precisely known, but it is used to identify gastrointestinal stromal tumors and solitary fibrous tumors.[33,34] It is also used to assess the degree of angiogenesis.[27,31-39] CD105 (endoglin) is a 180-kDa transmembrane glycoprotein, which is part of the transforming growth factor (TGF)-β receptor complex. It controls angiogenesis by controlling cellular proliferation, differentiation, and migration.[40] Unlike the VEGF or CD34, CD105 is weakly expressed in normal tissue and blood vessels but is strongly expressed in tumors.[40-42]

Immunohistochemical labeling for the proteins mentioned above is helpful for assessing the degree of angiogenesis in different model systems.[31,35,37-39,43-45] In the present study, we collected adipose tissue-derived stem cells from adult patients with liver disease, placed them in artificial scaffolds, and implanted these scaffolds in severe combined immunocompromised (SCID) mice to determine whether they induced angiogenesis.

MATERIALS AND METHODS

Experimental model

We employed SCID mice as an experimental model to study angiogenesis in transplanted bio-artificial liver models (Fig. 1). Four scaffolds were transplanted considering possible errors and effectiveness. Adipose tissue-derived stem cells from human patients were implanted into the artificial scaffolds made of type I collagen, and the scaffolds were implanted into the stomach surface of SCID mice. Tissues attached to and near the scaffolds were analyzed 30 days after implantation, which is reportedly a sufficient period of time for adequate angiogenesis.[46,47] The tissue was processed into frozen sections, and im-

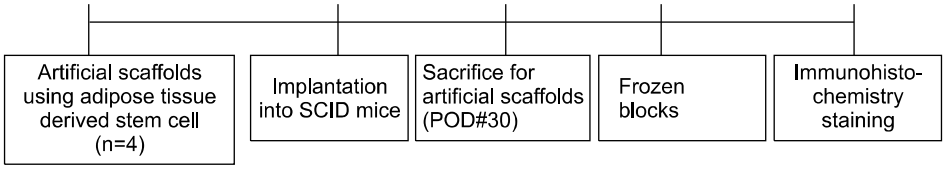

Fig. 1. Experimental model.

munohistochemistry labeling was performed to examine the expression of different angiogenesis markers.

Artificial scaffold production

Artificial scaffolds were comprised of adipose tissue-derived stem cells and type I collagen. Adult adipose cells were obtained from abdominal subcutaneous fat acquired during liver tumor resection from consenting patients, and the type I collagen was from pig skin. Harvest of tissues was performed under anesthesia according to procedures approved by the Institutional Review Board (IRB, 4-2013-0757) of Yonsei University Hospital, Korea. Type I collagen is the most abundant collagen in the human body, and it is a constituent of the extracellular matrix of internal organs such as the liver and spleen. Previous studies have shown that angiogenesis occurs through foreign body reaction;[46] therefore, type I collagen was considered the perfect material for artificial scaffolds in this experimental model. The model for the artificial scaffold was supplied by a Nanotechnology Laboratory at Yonsei University. An illustration of the artificial scaffold model is shown in Fig. 2.

Artificial scaffold implantation into SCID mice

The 12-week old male SCID mice (Charles River Laboratory, MA, USA) weighing ~20 g were used for the experiment. The study was carried out after receiving approval from the laboratory animal rule committee (animal experiment protocol number 2013-0346). Artificial scaffold implantation proceeded as follows. Anesthesia was induced by placing the animal in an inhalation chambers (RC2-rodent circuit controller, VetEquip, CA, USA) at inhalation level 4, and anesthesia was maintained at level 1.5-2 by placing an inhalation anesthetic tube near the animal's mouth. Under anesthesia, hair around the abdomen was removed, and the incision site at the left lateral decubitus position was disinfected with betadine. After making an incision in the subcostal area of the abdominal wall with surgical scissors, forceps were used to expose the stomach. Silicon tubes were used to scratch the stomach's surface, and the scaffolds were placed near the scratch. Vicryl 5-0 was used to fix the scaffolds by the fundus and pylorus of the stomach. The fixed artificial scaffolds were pressed into the abdominal cavity using cotton swabs, and the abdominal wall was sutured layer by layer using Vicryl 4-0. The anesthetic level was lowered during suturing to ensure a fast recovery of consciousness. The suture site was closely checked for 2-3 days after surgery.

Tissue processing

The specimens including the artificial scaffolds were removed 30 days after implantation to search for evidence of angiogenesis. They were immediately frozen after the mice were sacrificed. 12-μm thick tissue slices were processed from frozen blocks of tissue. The slides were stained with hematoxylin and eosin (H&E) to observe the general characteristics of the artificial scaffolds. To block endogenous peroxidase, the slides were immersed in 0.3% H_2O_2 solution for 5-10 minutes and then washed for 5 minutes in distilled water. Next, they were stained with hematoxylin for 5 minutes, washed with distilled water three times, washed with phosphate-buffered saline (PBS), immersed in ammonia for 1 minute, washed with distilled water 3 times, and immersed in eosin for 5 minutes. After

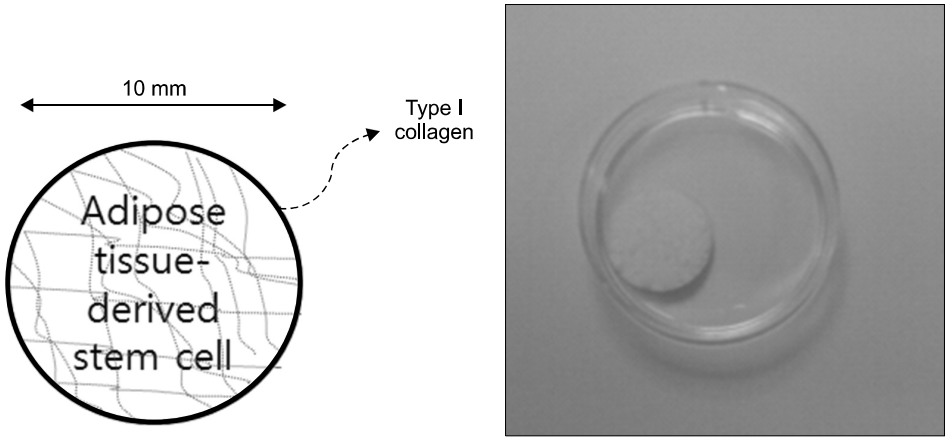

Fig. 2. Schematic presentation and a photograph of the artificial scaffold model.

2 minutes in 80% ethanol, 2 minutes in 100% ethanol, and 2 minutes in xylene, the slides were cover-slipped with Permount solution and observed under a light microscope (BX51, Olympus, Tokyo, Japan).

Known angiogenesis biomarkers (VEGF, CD34, and CD105) were immunohistochemically assessed. The frozen sections containing the artificial scaffolds and surrounding tissue were fixed for 5-10 minutes. To block endogenous peroxidase, the frozen sections were immersed in 0.3% hydrogen peroxide solution for 5-10 minutes and washed with distilled water for 5 minutes. Afterward, the blocks were placed a moist box and incubated at 4°C for a day with one of three primary antibodies directed against CD34, CD105, or VEGF (Table 1). Next, the sections were washed three times with PBS for 5 minutes each. Based on the visualization system instructions, the sections were incubated with secondary antibodies including anti-rabbit IgG (HRP) (sc-2749, Santa Cruz, CA, USA) and anti goat IgG (HRP) (sc-2741, Santa Cruz, CA, USA) at room temperature for 2 hours and then washed with PBS four times for 5 minutes each. The 1 : 250 diluted streptoavidin (DAKO, Glostrup, Denmark) reaction was carried out for more than 30 minutes, and then the blocks were washed with phosphate buffer saline (PBS) three times for 5 minutes each. Afterwards, the sections were chemically stained with the brown water-soluble dye diaminobenzidine (Vectorlabs, CA , USA) After washing with distilled water, the sections were incubated with hematoxylin for counterstaining. After a final wash in flowing distilled water, the slides were immersed for 10 minutes in PBS. For dehydration and mounting, the blocks were immersed in 95% alcohol for 2 minutes followed by xylene for 2 minutes. The slides were then cover-slipped with Permount solution and examined under a microscope.

Table 1. Antibodies used for immunohistochemistry*

Antibody	Dilution	Incubation	Origin
Monoclonal CD 34	1 : 200	Overnight	Goat
Monoclonal CD105	1 : 200	Overnight	Rabbit
Polyclonal VEGF	1 : 200	Overnight	Rabbit

*All antibodies were purchased from Santa Cruz Biotechnology (Santa Cruz, CA, USA)

RESULTS

Gross findings

The gross findings in mice that were sacrificed and dissected 30 days after artificial scaffold implantation are shown in Fig. 3. The artificial scaffolds were covered with the omentum and adhered to the fundus and pylorus suture areas, as well as to the surrounding organs.

H&E staining

We observed the H&E-stained artificial scaffolds under low magnification to assess their overall appearance. Fig. 4 shows collagen surrounding the scaffold that contained adipose tissue-derived stem cells. The collagen membrane

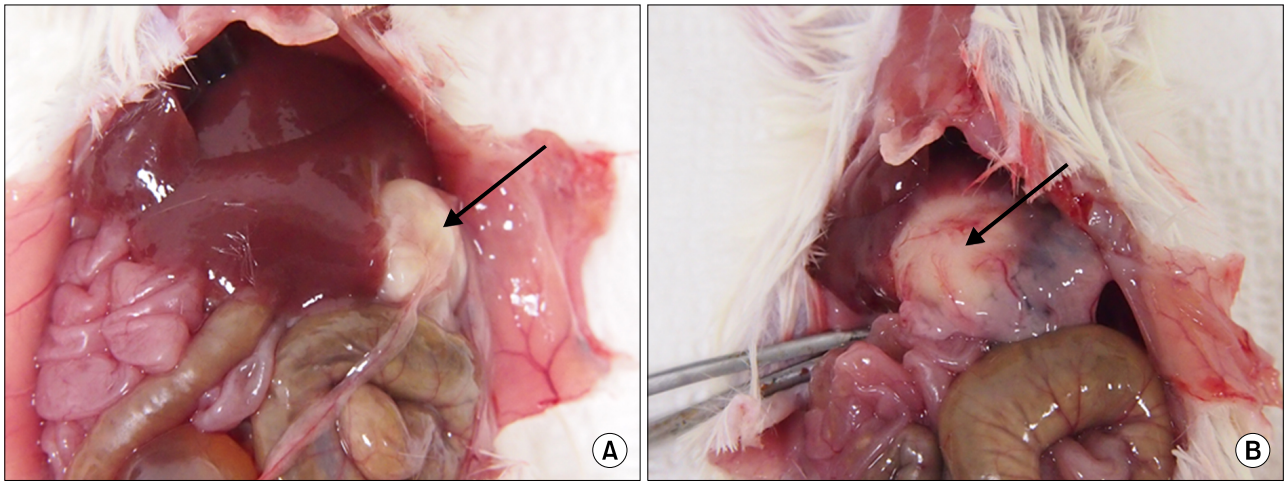

Fig. 3. Adhesion of artificial scaffold to surrounding organs 30 days after implantation into SCID mice. (A) View of internal organs after opening the mouse abdomen. (B) The artificial scaffold (black arrow) was exposed with surgical forceps. The omentum was covering the artificial scaffold.

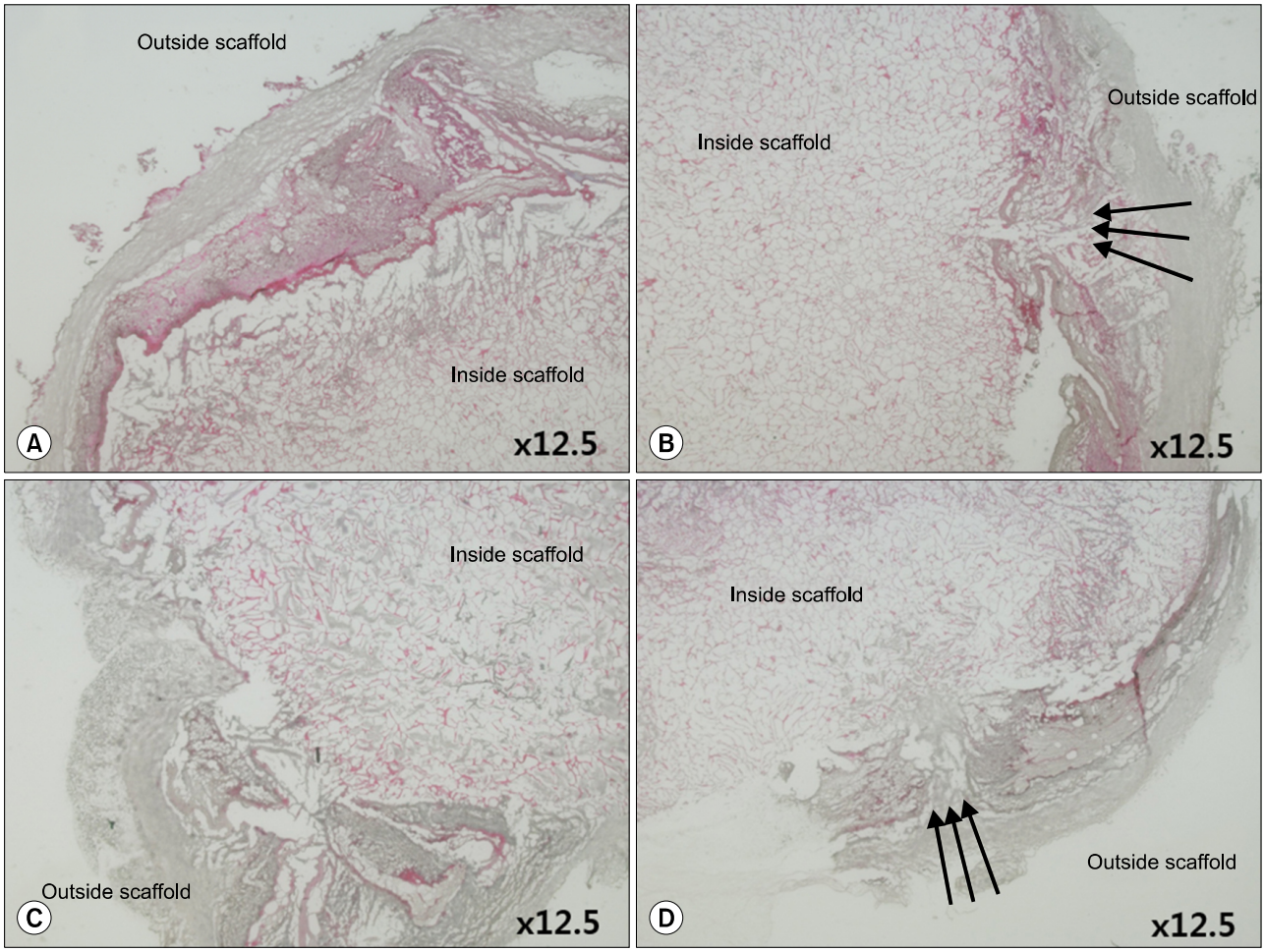

Fig. 4. H&E-stained images of the artificial scaffold material processed 30 days after implantation into SCID mice. Red eosin stain showed the artificial collagen scaffold. Black arrows indicate where the scaffold was sutured to the mouse stomach.

was disrupted where the scaffold was sutured to fix it to the pylorus and fundus, and this membrane linked the artificial scaffold and the stomach.

We next observed the H&E-stained artificial scaffolds under high magnification to better assess its characteristics (Figs. 5, 6). The basement membrane surrounding the outer side of the artificial scaffold contained eosin-stained collagen without nuclei (Fig. 5), and we also observed hematoxylin-stained adipose tissue-derived stem cells within the artificial scaffold (Fig. 6).

Immunohistochemistry with VEGF, CD34, CD105

VEGF-labeled slides showed brown staining starting from the membrane of the artificial scaffold (Fig. 7A, B), but there was no evidence of endothelial cells or vascular structure at ×200 magnification. Although collagen was stained brown by diaminobenzidine, the inside of the cells were not positive for VEGF (Fig. 7E, F).

The inside and outside of the artificial membrane were assessed under high magnification to view cell shapes and differences in VEGF immunohistochemistry. Mouse omentum cells were observed outside the scaffold, and there was no positive staining for VEGF (Fig. 7E). The inside of the artificial scaffold contained hematoxylin-stained adipose tissue-derived stem cells and diaminobenzidine-stained collagen but was negative for VEGF (Fig. 7F).

CD34-labeled slides also showed progressive brown stain starting from the membrane of the artificial scaffold (Fig. 8A, B), but again there was no sign of endothelial cells or vascular structures at ×200 magnification, and the inside of cells were negative for CD34 expression (Fig. 8D, E). Both the inside and outside of the artificial scaffold were checked under high magnification in order to see the cell shape and difference in CD34 immunohistochemistry

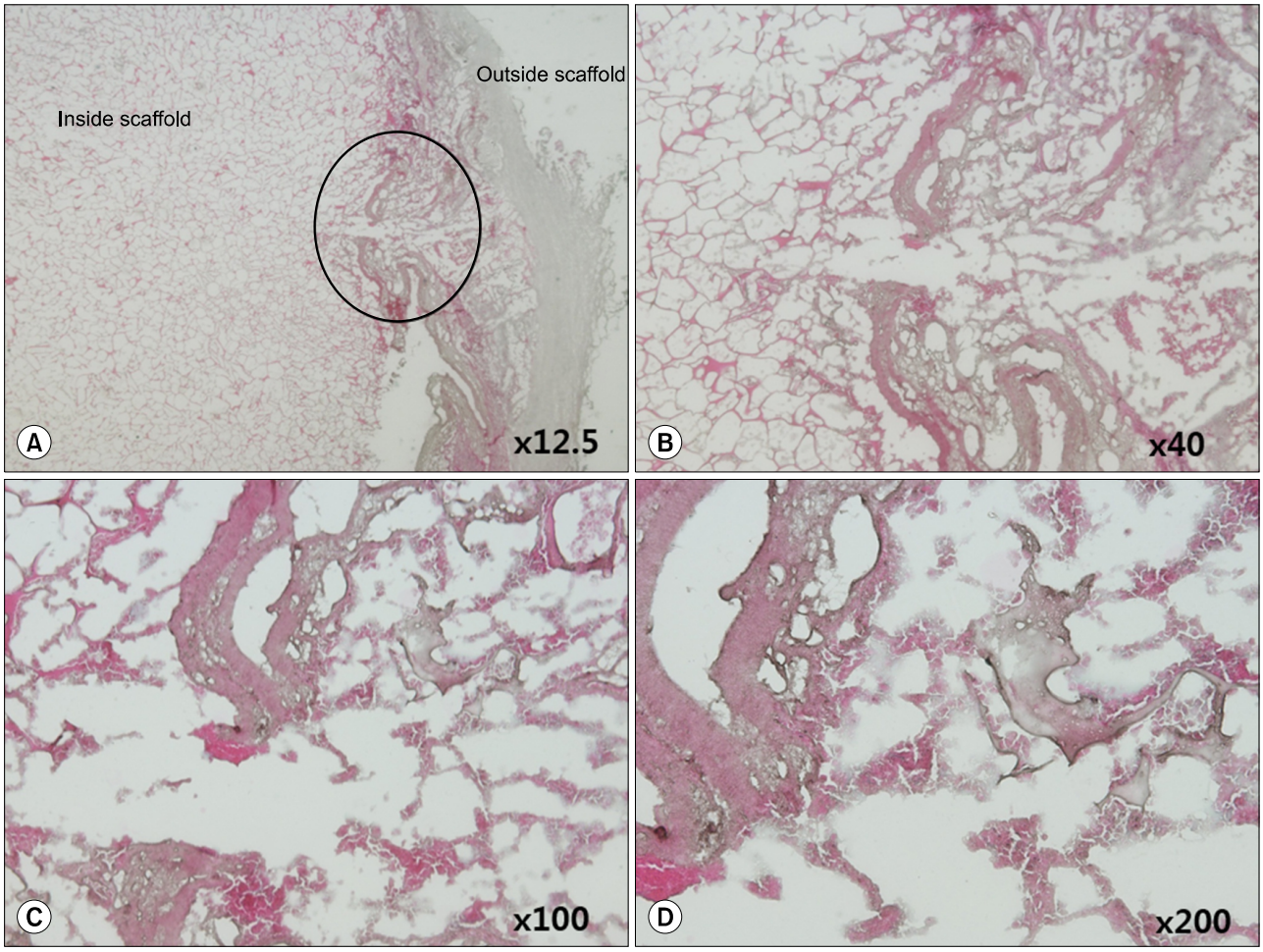

Fig. 5. H&E-stained collagen of the artificial scaffold 30 days after implantation into SCID mice. The area in the black circle (A) is magnified in (B-D). (D) The ×200 magnification shows the lack of nuclei in the red eosin-stained collagen surrounding the artificial scaffold.

staining. Mouse omentum cells were observed outside the scaffold, and there was no positive staining for CD34 (Fig. 8E). The inside of the artificial scaffold contained hematoxylin-stained adipose tissue-derived stem cells and diaminobenzidine-stained collagen but was negative for CD34 (Fig. 8F).

The CD105 immunohistochemistry stained slide also showed progressive brown staining starting from the membrane of the artificial scaffold (Fig. 9A, B). There were no endothelial cells or vascular structures at ×200 magnification, and the inside of the scaffold contained only stained collagen and was negative for CD105. Mouse omentum cells were observed outside the scaffold, and there was no positive staining for CD105 (Fig. 9E). On the other hand, the inside of the artificial scaffold contained hematoxylin-stained adipose tissue-derived stem cells and diaminobenzidine-stained collagen but was negative for CD105 (Fig. 9F). Microscopic observation failed to reveal any endothelial cells or vascular structures within the artificial scaffolds. Although diaminobenzidine-stained brown collagen was visible inside the scaffolds, the three angiogenesis markers were not expressed.

DISCUSSION

In the past 20 years, most tissue engineering projects have employed thin structures such as skin or vesical arteries.[48-50] Manufacturing thick tissues such as muscle, liver, and kidney on scaffolds was not considered possible due to insufficient diffusion of oxygen and nutrients.[51] To overcome this problem, the pig liver experimental model was developed by removing most of the cells and only

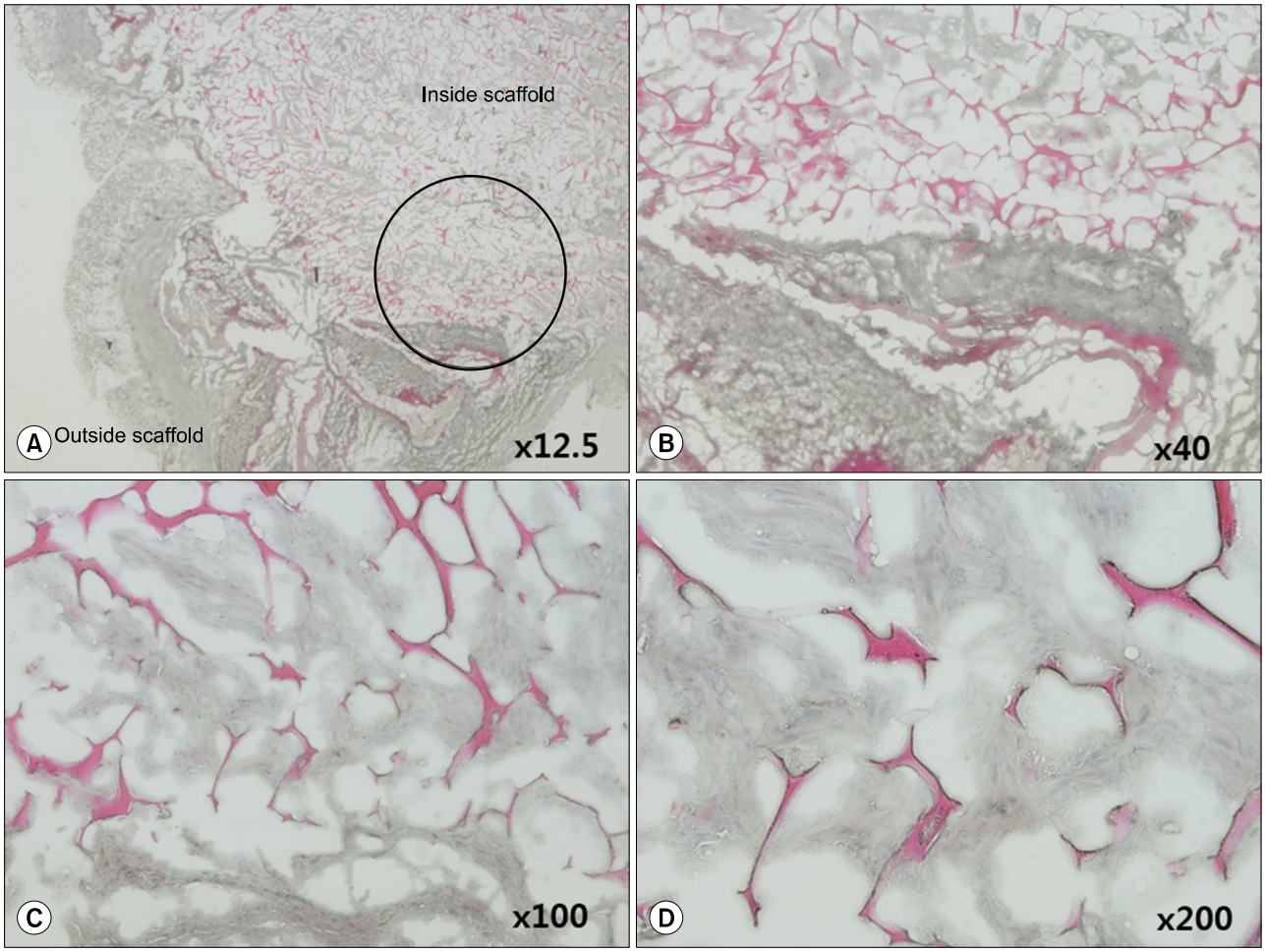

Fig. 6. Magnification of the inner side of the H&E-stained artificial scaffold 30 days after implantation into SCID mice. The area in the black circle (A) is magnified in (B-D). (D) The ×200 magnification shows eosin-stained collagen and hematoxylin-stained adipose tissue-derived stem cells within the artificial scaffold.

leaving the vessels with mechanical perfusion. Still, microfilaments and microtubules were damaged in the process.[52]

In the present study, we designed an experimental model under the assumption that vessels from the omentum will grow into the artificial scaffolds implanted onto the vessel-rich mouse stomach. In general, active liver regeneration occurs for 7 days after liver resection in mice, and most show regeneration within a month.[53] Previous studies reported that 30 days is a sufficient period of time for angiogenesis to occur. Therefore, we carried performed immunohistochemical labeling 1 month after artificial scaffold implantation. We expected to observe angiogenesis in the artificial scaffolds, but light microscopy of H&E-stained and antibody-labeled sections failed to reveal any evidence of angiogenesis.

There were diaminobenzidine-stained brown regions indicating that there could be transport of materials involved in angiogenesis from outside the artificial scaffold to inside. Specifically, the suture sites where the artificial scaffolds were fixed onto the mice appeared to contain connecting tracts. However, if there was angiogenesis from outside the artificial scaffolds, there would be evidence of endothelial cells or tubular structures inside the scaffolds, and these changes were not observed. In addition, only collagen was stained by diaminobenzidine; there was no evidence of angiogenesis marker expression.

There are several possible reasons why we were unable to find evidences of angiogenesis markers. First, previous studies used 12 weeks old C57bl/6 male mice, whereas we used SCID mice to prevent a reaction to the implanted adipose-derived stem cells. While our animal model choice might have helped maintain the adipose-derived stem cells

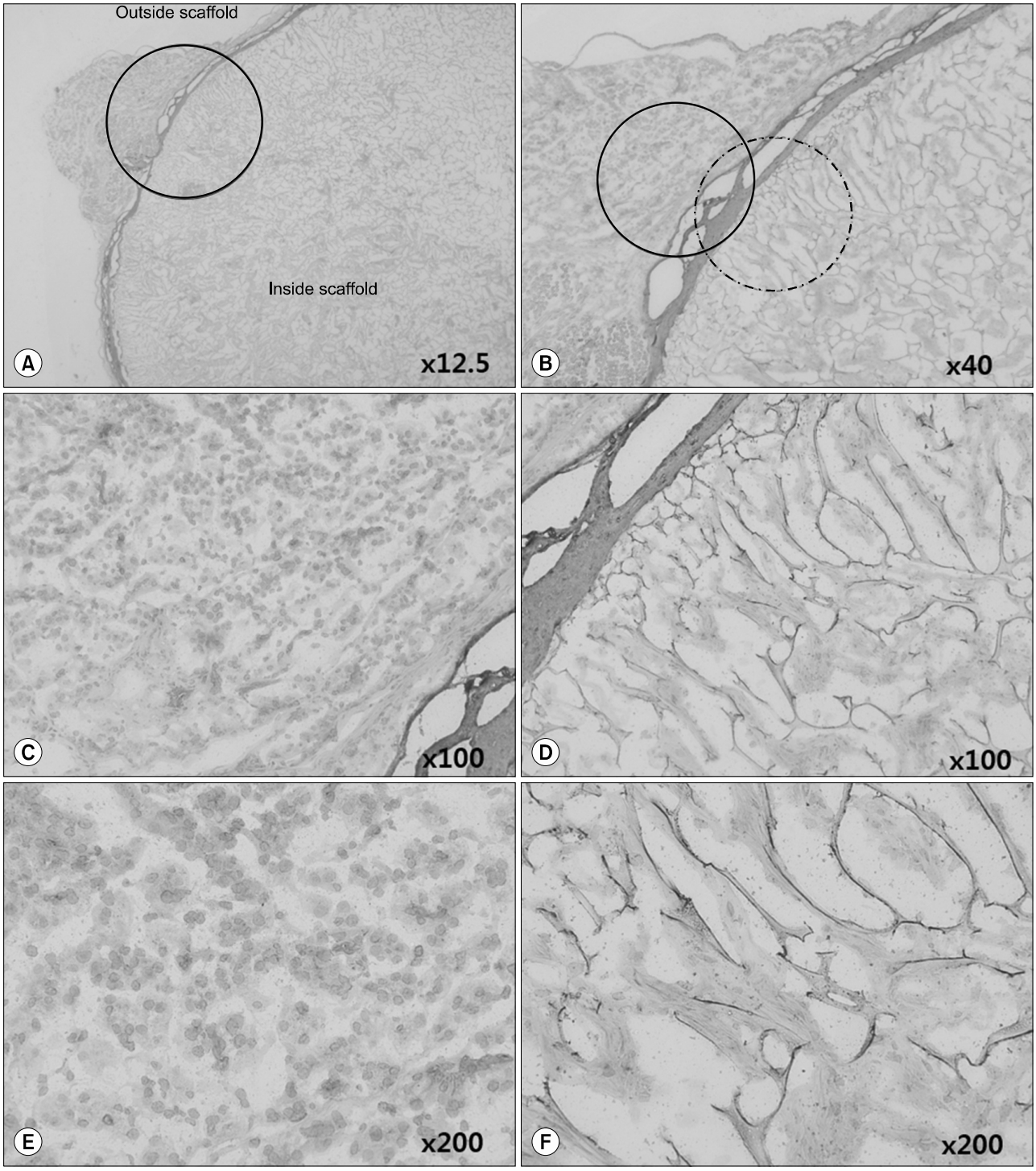

Fig. 7. A VEGF-stained artificial scaffold processed 30 days after implantation into SCID mice. The area in the black circle (A) is magnified. (D) ×100 and (F) ×200 magnifications of the area in the black dotted circle shown in (B). The cells inside the artificial scaffold include hematoxylin-stained adipose tissue-derived stem cells and diaminobenzidine-stained collagen. (C) ×100 magnification and (E) ×200 magnification of the area in the black circle shown in (B). The outside of the artificial scaffold contained mouse omentum cells with no collagen. There was no endothelial or vascular structure or VEGF expression.

within the artificial scaffolds, it also could have been an obstacle preventing foreign body reaction and angiogenesis. Secondly, it is possible that the type I collagen scaffolds were not appropriate for inducing angiogenesis. But as van Amerongen et al. reported, angiogenesis occurred through foreign body reaction 7 days after the implantation of type

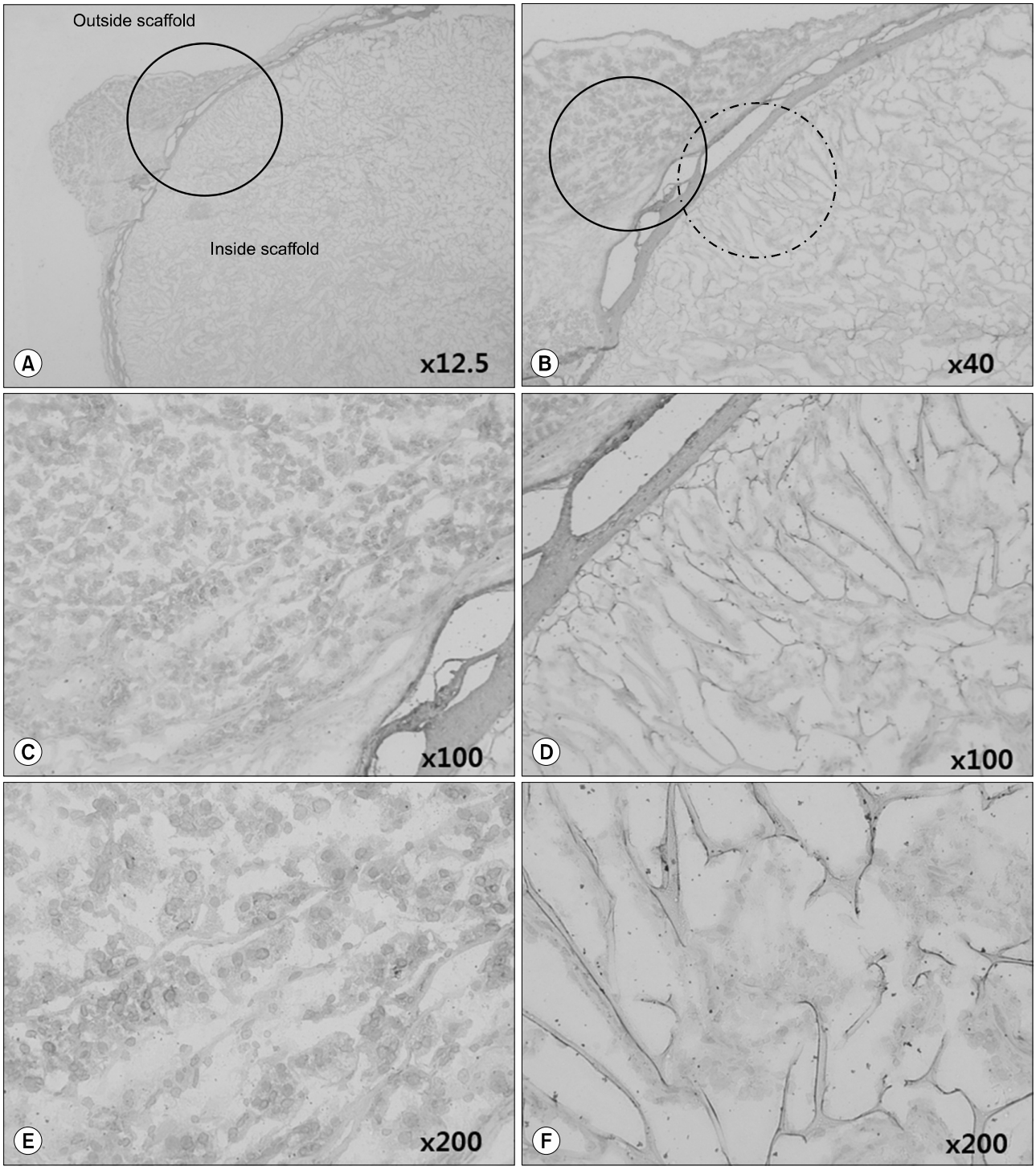

Fig. 8. A CD34-stained artificial scaffold processed 30 days after implantation into SCID. The area in the black circle (A) is magnified. (D) ×100 and (F) ×200 magnifications of the area in the black dotted circle area (B). The cells inside the artificial scaffold include hematoxylin-stained adipose tissue-derived stem cells and diaminobenzidine-stained collagen. (C) ×100 magnification and (E) ×200 magnification of the area in the black circle shown in (B). The outside of the artificial scaffold contained mouse omentum cells with no collagen. There was no endothelial or vascular structure or CD34 expression.

I collagen into mice.[46] Thirdly, our time points may have been too short, even though previous studies have shown that angiogenesis starts as early as 7 days after implantation and is clearly observed within 14 and 30 days.[46,47] For a more appropriate comparison, it would have been better to have a comparison group of scaffold removal at 90 or

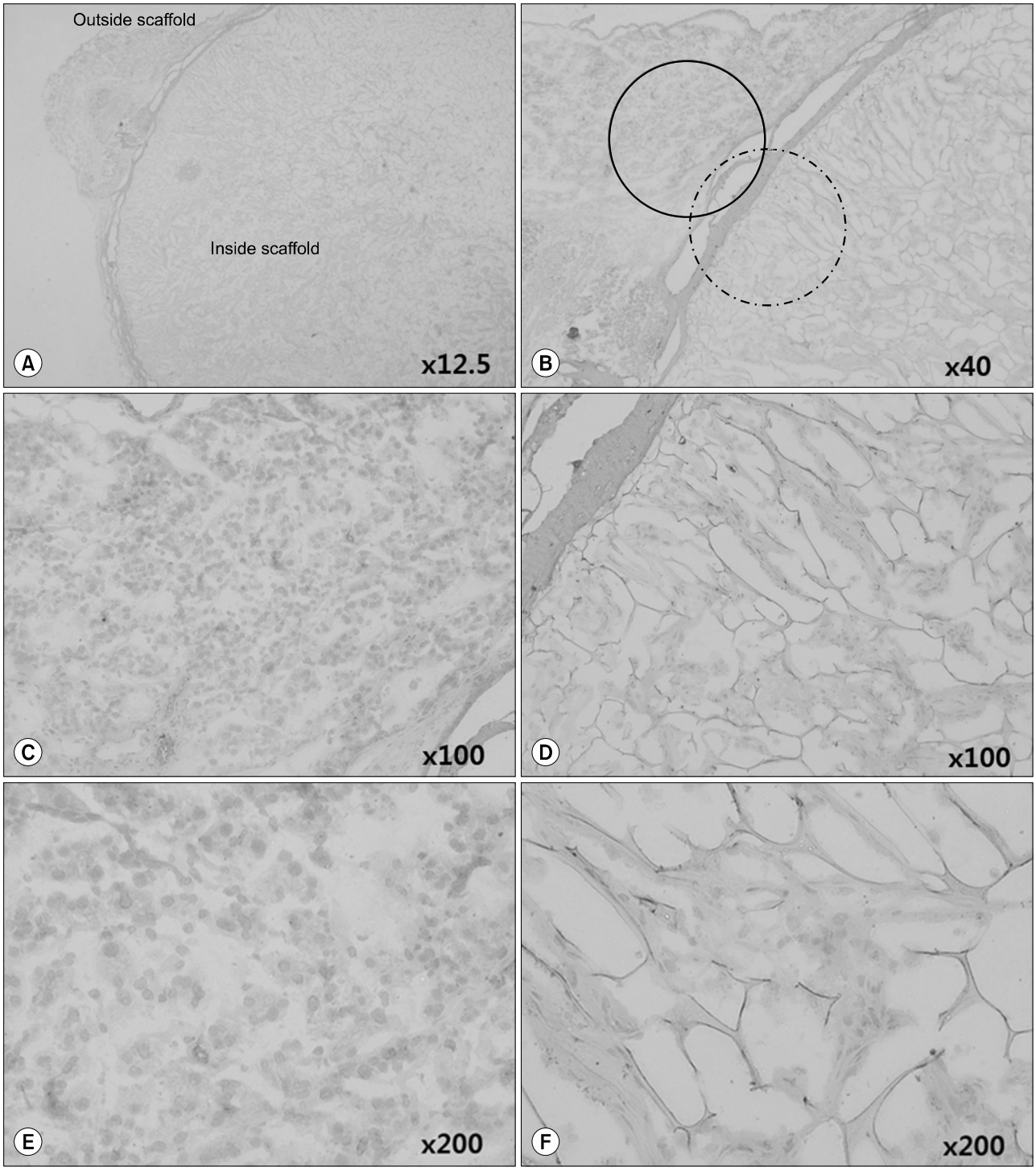

Fig. 9. A CD105-stained artificial scaffold processed 30 days after implantation into SCID. The area in the black circle (A) is magnified. (D) ×100 and (F) ×200 magnifications of the area in the black dotted circle area (B). The cells inside the artificial scaffold include hematoxylin-stained adipose tissue-derived stem cells and diaminobenzidine-stained collagen. (C) ×100 magnification and (E) ×200 magnification of the area in the black circle shown in (B). The outside of the artificial scaffold contained mouse omentum cells with no collagen. There was no endothelial or vascular structure or CD105 expression.

180 days.

If our second presumption is correct, it would indicate that artificial scaffolds made with type I collagen do not elicit sufficient tissue reaction. Although there might be adhesion to surrounding tissue, the implanted cells are maintained without angiogenesis, and this suggests that

type I collagen artificial scaffolds are an acceptable biomaterial for transplantation. Additional experiments on normal mice are needed to provide additional support for this theory.

In conclusion, there was no evidence of angiogenesis in the artificial scaffolds comprised of type I collagen 30 days after implantation. Similarly, we did not observe endothelial cells or angiogenesis markers. Although the results were negative, they do indicate that such scaffolds could be useful as a new biomaterial. Scaffolds made with type I collagen induced minimal tissue reactions and could maintain implanted cells. Additional research is needed to assess their utility in transplantation.

ACKNOWLEDGEMENTS

This research was supported by Basic Science Research Program through the National Research Foundation of Korea (NRF) funded by the Ministry of Education (2012R1A1A2006942).

REFERENCES

1. Korean Network for Organ Sharing. Annual Report of the transplant 2013. Ministry of Welfare, 2014.
2. Dutkowski P, Oberkofler CE, Béchir M, Müllhaupt B, Geier A, Raptis DA, et al. The model for end-stage liver disease allocation system for liver transplantation saves lives, but increases morbidity and cost: a prospective outcome analysis. Liver Transpl 2011; 17:674-684.
3. Axelrod DA. Economic and financial outcomes in transplantation: whose dime is it anyway? Curr Opin Organ Transplant 2013;18: 222-228.
4. Dutkowski P, Oberkofler CE, Slankamenac K, Puhan MA, Schadde E, Müllhaupt B, et al. Are there better guidelines for allocation in liver transplantation? A novel score targeting justice and utility in the model for end-stage liver disease era. Ann Surg 2011;254:745-753.
5. Struecker B, Raschzok N, Sauer IM. Liver support strategies: cutting-edge technologies. Nat Rev Gastroenterol Hepatol 2014; 11:166-176.
6. Iwata H, Ueda Y. Pharmacokinetic considerations in development of a bioartificial liver. Clin Pharmacokinet 2004;43:211-225.
7. Sauer IM, Kardassis D, Zeillinger K, Pascher A, Gruenwald A, Pless G, et al. Clinical extracorporeal hybrid liver support--phase I study with primary porcine liver cells. Xenotransplantation 2003;10:460-469.
8. Pascher A, Sauer IM, Neuhaus P. Analysis of allogeneic versus xenogeneic auxiliary organ perfusion in liver failure reveals superior efficacy of human livers. Int J Artif Organs 2002;25: 1006-1012.
9. Laconi E, Oren R, Mukhopadhyay DK, Hurston E, Laconi S, Pani P, et al. Long-term, near-total liver replacement by transplantation of isolated hepatocytes in rats treated with retrorsine. Am J Pathol 1998;153:319-329.
10. Dhawan A, Strom SC, Sokal E, Fox IJ. Human hepatocyte transplantation. Methods Mol Biol 2010;640:525-534.
11. Gupta S, Rajvanshi P, Sokhi R, Slehria S, Yam A, Kerr A, et al. Entry and integration of transplanted hepatocytes in rat liver plates occur by disruption of hepatic sinusoidal endothelium. Hepatology 1999;29:509-519.
12. Ambrosino G, Varotto S, Strom SC, Guariso G, Franchin E, Miotto D, et al. Isolated hepatocyte transplantation for Crigler-Najjar syndrome type 1. Cell Transplant 2005;14:151-157.
13. Darwish AA, Sokal E, Stephenne X, Najimi M, de Goyet Jde V, Reding R. Permanent access to the portal system for cellular transplantation using an implantable port device. Liver Transpl 2004;10:1213-1215.
14. Dhawan A, Mitry RR, Hughes RD. Hepatocyte transplantation for liver-based metabolic disorders. J Inherit Metab Dis 2006;29: 431-435.
15. Allen KJ, Mifsud NA, Williamson R, Bertolino P, Hardikar W. Cell-mediated rejection results in allograft loss after liver cell transplantation. Liver Transpl 2008;14:688-694.
16. Lysy PA, Najimi M, Stephenne X, Bourgois A, Smets F, Sokal EM. Liver cell transplantation for Crigler-Najjar syndrome type I: update and perspectives. World J Gastroenterol 2008;14: 3464-3470.
17. Kriks S, Shim JW, Piao J, Ganat YM, Wakeman DR, Xie Z, et al. Dopamine neurons derived from human ES cells efficiently engraft in animal models of Parkinson's disease. Nature 2011; 480:547-551.
18. Kroon E, Martinson LA, Kadoya K, Bang AG, Kelly OG, Eliazer S, et al. Pancreatic endoderm derived from human embryonic stem cells generates glucose-responsive insulin-secreting cells in vivo. Nat Biotechnol 2008;26:443-452.
19. Si-Tayeb K, Noto FK, Nagaoka M, Li J, Battle MA, Duris C, et al. Highly efficient generation of human hepatocyte-like cells from induced pluripotent stem cells. Hepatology 2010;51:297-305.
20. Han HS, Ahn KS, Cho JY, Yoon YS, Yoon CJ, Park KU, et al. Autologous stem cell transplantation for expansion of remnant liver volume with extensive hepatectomy. Hepatogastroenterology 2014;61:156-161.
21. Moon JJ, West JL. Vascularization of engineered tissues: approaches to promote angio-genesis in biomaterials. Curr Top Med Chem 2008;8:300-310.
22. Weis SM, Cheresh DA. Tumor angiogenesis: molecular pathways and therapeutic targets. Nat Med 2011;17:1359-1370.
23. Kim YW, Byzova TV. Oxidative stress in angiogenesis and vascular disease. Blood 2014;123:625-631.
24. Crafts TD, Jensen AR, Blocher-Smith EC, Markel TA. Vascular endothelial growth factor: therapeutic possibilities and challenges for the treatment of ischemia. Cytokine 2015;71:385-393.
25. West CM, Cooper RA, Loncaster JA, Wilks DP, Bromley M. Tumor vascularity: a histological measure of angiogenesis and hypoxia. Cancer Res 2001;61:2907-2910.
26. Kaully T, Kaufman-Francis K, Lesman A, Levenberg S. Vascularization--the conduit to viable engineered tissues. Tissue Eng Part B Rev 2009;15:159-169.
27. Li LH, Guo ZJ, Yan LL, Yang JC, Xie YF, Sheng WH, et al. Antitumor and antiangiogenic activities of anti-vascular endothelial growth factor hairpin ribozyme in human hepatocellular carcinoma cell cultures and xenografts. World J Gastroenterol 2007; 13:6425-6432.
28. Ng YS, Krilleke D, Shima DT. VEGF function in vascular pathogenesis. Exp Cell Res 2006;312:527-537.
29. Maharaj AS, D'Amore PA. Roles for VEGF in the adult. Microvasc Res 2007;74:100-113.

30. Holmes K, Roberts OL, Thomas AM, Cross MJ. Vascular endothelial growth factor receptor-2: structure, function, intracellular signalling and therapeutic inhibition. Cell Signal 2007;19:2003-2012.
31. Pisacane AM, Picciotto F, Risio M. CD31 and CD34 expression as immunohistochemical markers of endothelial transdifferentiation in human cutaneous melanoma. Cell Oncol 2007;29:59-66.
32. Pusztaszeri MP, Seelentag W, Bosman FT. Immunohistochemical expression of endothelial markers CD31, CD34, von Willebrand factor, and Fli-1 in normal human tissues. J Histochem Cytochem 2006;54:385-395.
33. Westra WH, Gerald WL, Rosai J. Solitary fibrous tumor. Consistent CD34 immunoreactivity and occurrence in the orbit. Am J Surg Pathol 1994;18:992-998.
34. Kutzner H. Expression of the human progenitor cell antigen CD34 (HPCA-1) distinguishes dermatofibrosarcoma protuberans from fibrous histiocytoma in formalin-fixed, paraffin-embedded tissue. J Am Acad Dermatol 1993;28:613-617.
35. Vasconcelos MG, Alves PM, Vasconcelos RG, da Silveira ÉJ, Medeiros AM, de Queiroz LM. Expression of CD34 and CD105 as markers for angiogenesis in oral vascular malformations and pyogenic granulomas. Eur Arch Otorhinolaryngol 2011;268: 1213-1217.
36. Popa ER, Harmsen MC, Tio RA, van der Strate BW, Brouwer LA, Schipper M, et al. Circulating CD34+ progenitor cells modulate host angiogenesis and inflammation in vivo. J Mol Cell Cardiol 2006;41:86-96.
37. Vieira SC, Silva BB, Pinto GA, Vassallo J, Moraes NG, Santana JO, et al. CD34 as a marker for evaluating angiogenesis in cervical cancer. Pathol Res Pract 2005;201:313-318.
38. Kimura H, Nakajima T, Kagawa K, Deguchi T, Kakusui M, Katagishi T, et al. Angiogenesis in hepatocellular carcinoma as evaluated by CD34 immunohistochemistry. Liver 1998;18:14-19.
39. Karavasilis V, Malamou-Mitsi V, Briasoulis E, Tsanou E, Kitsou E, Kalofonos H, et al. Angiogenesis in cancer of unknown primary: clinicopathological study of CD34, VEGF and TSP-1. BMC Cancer 2005;5:25.
40. Fonsatti E, Maio M. Highlights on endoglin (CD105): from basic findings towards clinical applications in human cancer. J Transl Med 2004;2:18.
41. Fonsatti E, Del Vecchio L, Altomonte M, Sigalotti L, Nicotra MR, Coral S, et al. Endoglin: An accessory component of the TGF-beta-binding receptor-complex with diagnostic, prognostic, and bioimmunotherapeutic potential in human malignancies. J Cell Physiol 2001;188:1-7.
42. Sharma S, Sharma MC, Sarkar C. Morphology of angiogenesis in human cancer: a conceptual overview, histoprognostic perspective and significance of neoangiogenesis. Histopathology 2005;46:481-489.
43. Wang D, Stockard CR, Harkins L, Lott P, Salih C, Yuan K, et al. Immunohistochemistry in the evaluation of neovascularization in tumor xenografts. Biotech Histochem 2008;83:179-189.
44. Farrell DJ, Bulmer E, Angus B, Ashcroft T. Immunohistochemical expression of endothelial markers in left atrial myxomas: a study of six cases. Histopathology 1996;28:147-152.
45. Kademani D, Lewis JT, Lamb DH, Rallis DJ, Harrington JR. Angiogenesis and CD34 expression as a predictor of recurrence in oral squamous cell carcinoma. J Oral Maxillofac Surg 2009; 67:1800-1805.
46. van Amerongen MJ, Molema G, Plantinga J, Moorlag H, van Luyn MJ. Neovascularization and vascular markers in a foreign body reaction to subcutaneously implanted degradable biomaterial in mice. Angiogenesis 2002;5:173-180.
47. Du C, Narayanan K, Leong MF, Wan AC. Induced pluripotent stem cell-derived hepatocytes and endothelial cells in multi-component hydrogel fibers for liver tissue engineering. Biomaterials 2014;35:6006-6014.
48. Zacchi V, Soranzo C, Cortivo R, Radice M, Brun P, Abatangelo G. In vitro engineering of human skin-like tissue. J Biomed Mater Res 1998;40:187-194.
49. Kaushal S, Amiel GE, Guleserian KJ, Shapira OM, Perry T, Sutherland FW, et al. Functional small-diameter neovessels created using endothelial progenitor cells expanded ex vivo. Nat Med 2001;7:1035-1040.
50. Hakenberg OW. Re: tissue-engineered autologous bladders for patients needing cystoplasty. Eur Urol 2006;50:382-383.
51. Griffith LG, Naughton G. Tissue engineering--current challenges and expanding opportunities. Science 2002;295:1009-1014.
52. Sano MB, Neal RE 2nd, Garcia PA, Gerber D, Robertson J, Davalos RV. Towards the creation of decellularized organ constructs using irreversible electroporation and active mechanical perfusion. Biomed Eng Online 2010;9:83.
53. Maruyama H, Harada A, Kurokawa T, Kobayashi H, Nonami T, Nakao A, et al. Duration of liver ischemia and hepatic regeneration after hepatectomy in rats. J Surg Res 1995;58:290-294.